PNAS
www.pnas.org

Supplementary Information for

Complex Mortuary Dynamics in the Upper Paleolithic of the Decorated Grotte de Cussac, France

Sacha Kacki, Erik Trinkaus, Eline M. J. Schotsmans, Patrice Courtaud, Irene Dori, Bruno Dutailly, Pierre Guyomarc'h, Pascal Mora, Vitale S. Sparacello, Sébastien Villotte

This PDF File Includes:

Supplementary text SI-1 to SI-6
Figures S1 to S17
Tables S1 to S13
References 1 to 19 for Supporting Information References

SI-1. Investigation Conditions and Procedures

Given the exceptional nature of the Grotte de Cussac, the cave was classified as a National Heritage site in 2002 (1). It is therefore subject to strict conservation measures. The cave is closed to visits except for scientific investigations, and access is limited due to health hazards to the periods when the partial pressure of carbon dioxide in the cave is below 2%. The scientific team is required to use artificial platforms and follow marked paths, in order to maximize the preservation of the cave floors. No conventional archaeological investigation is currently allowed, and only minor disturbances of the surface and its remains (see below) have been allowed in the past.

These specific study conditions in Cussac drastically limit the analyses that can be performed on the bioanthropological material (2–4). A significant portion of human remains are

www.pnas.org/cgi/doi/10.1073/pnas.2005242117

located several meters away from the authorized paths. Hence, their analysis is restricted to remote visual observations and to the study of photographs, both limited by several factors: limited (all artificial) light, extensive viewing distance for some clusters of remains, and bones partially or totally covered with sediment.

Observations and photographic acquisitions

Visual observations have been made on a yearly basis by the bioanthropological team, usually every January since the creation of the *Projet Collectif de Recherche* (Joint Research Program) in 2010. The different loci where bones can be found were photographed from as many different angles as possible in order to determine more precisely the natures of the fragments, but also to compute high definition 3D photogrammetric models.

Locus 1

The two main areas with human remains, Depressions 2 and 3, are ca. 2.75 m from the pathway, which makes observations very difficult and necessarily limited (Fig. S1). Pictures, including close up views of the human remains, were taken using a telescopic pole.

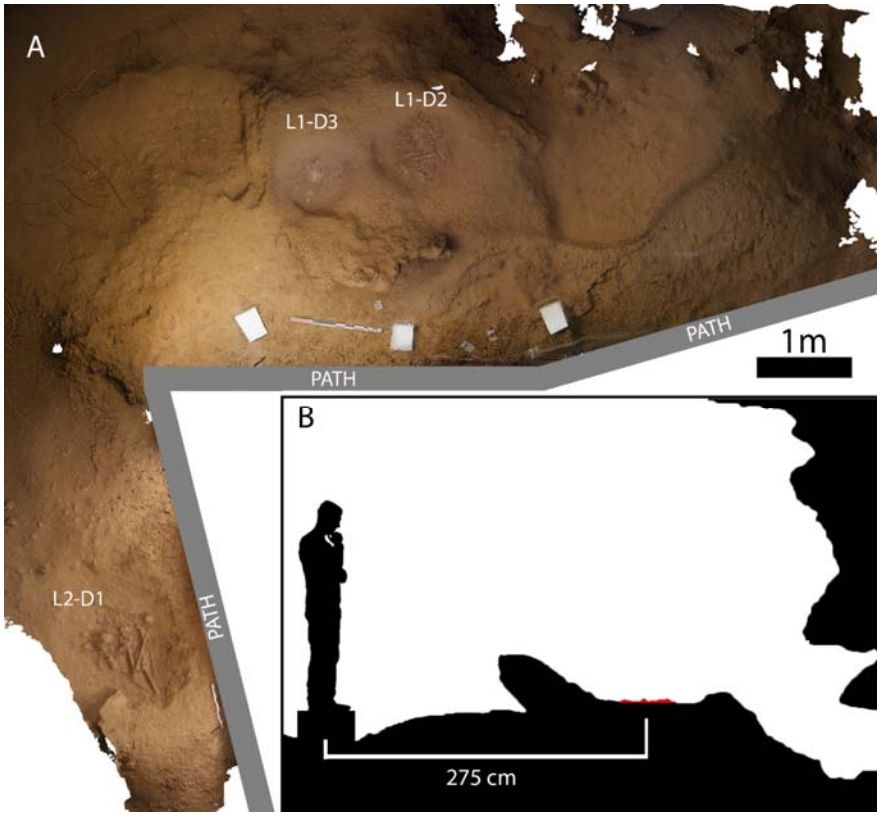

Figure S1. A) Orthoplane computed from the global 3D model of the Loci 1 and 2. B) Profile plane through the path and the Depression L1-D2, created from the global 3D model of Loci 1 and 2. The bone accumulation in the depression is indicated in red.

Locus 2

Locus 2-D1 is relatively close to the path used by the scientific team. The adjacent path is via a narrow passage, thanks in part to the metallic walkway that passes ca. 40 cm from the Locus. In 2013, an extension of the walkway was mounted directly above Locus 2, allowing for closer observations (Fig. S2). However, all of the bones in L2-D1 are covered by fine grained sediment. The layer of sediment fits very closely to the forms of the bones, but thicknesses range from several millimeters to more than in a centimeter in some areas (see below and 1), which limits greatly the observations that can be made *in situ*. Pictures were taken from the metallic walkway and the extension, before and after the local removing of sediment (see below) (Fig. S2).

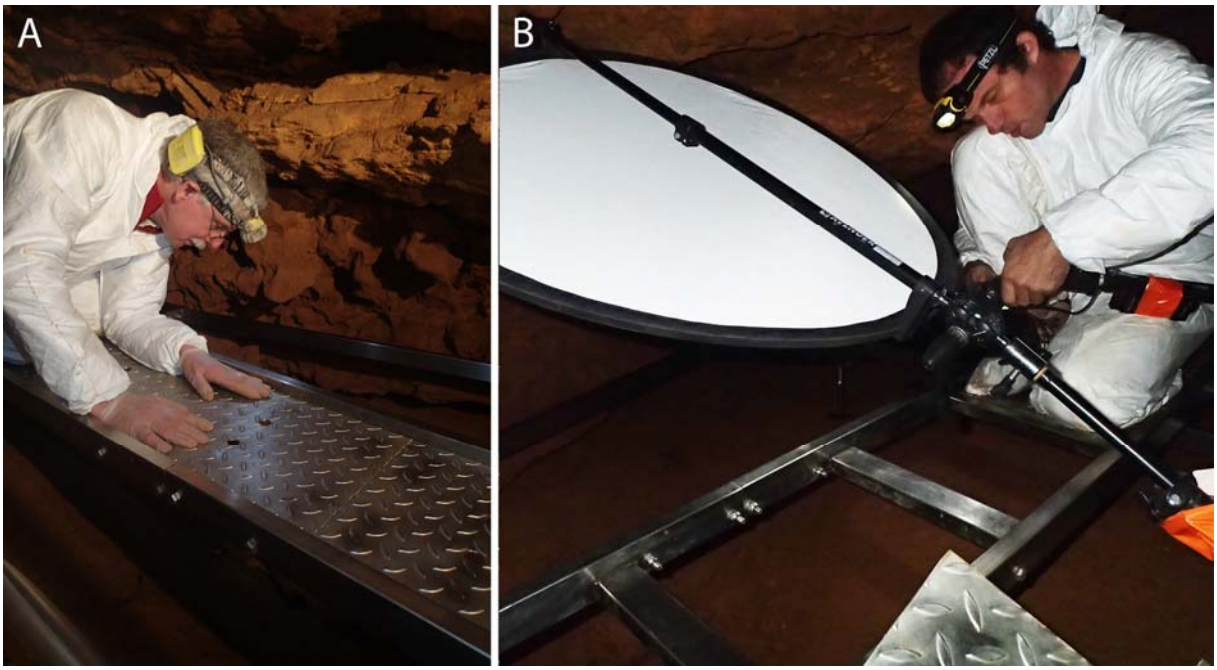

Figure S2. Observations (A) and photographic acquisitions (B) from the extension directly above Locus 2.

Locus 3

Locus 3 consists of a vast area of ca. 15 square meters with a complex topography, located in a cave meander. Most of the area is occupied by a massif of cave sediment associated with a large stalagmitic mass (Fig. S3). As with Locus 1, direct observations of the bones down the slopes around the stalagmites are made from the pathway, from a distance of 1 to 3 m. Similarly to Locus 1, a photographic survey has been carried out using a telescopic pole (Fig. S3).

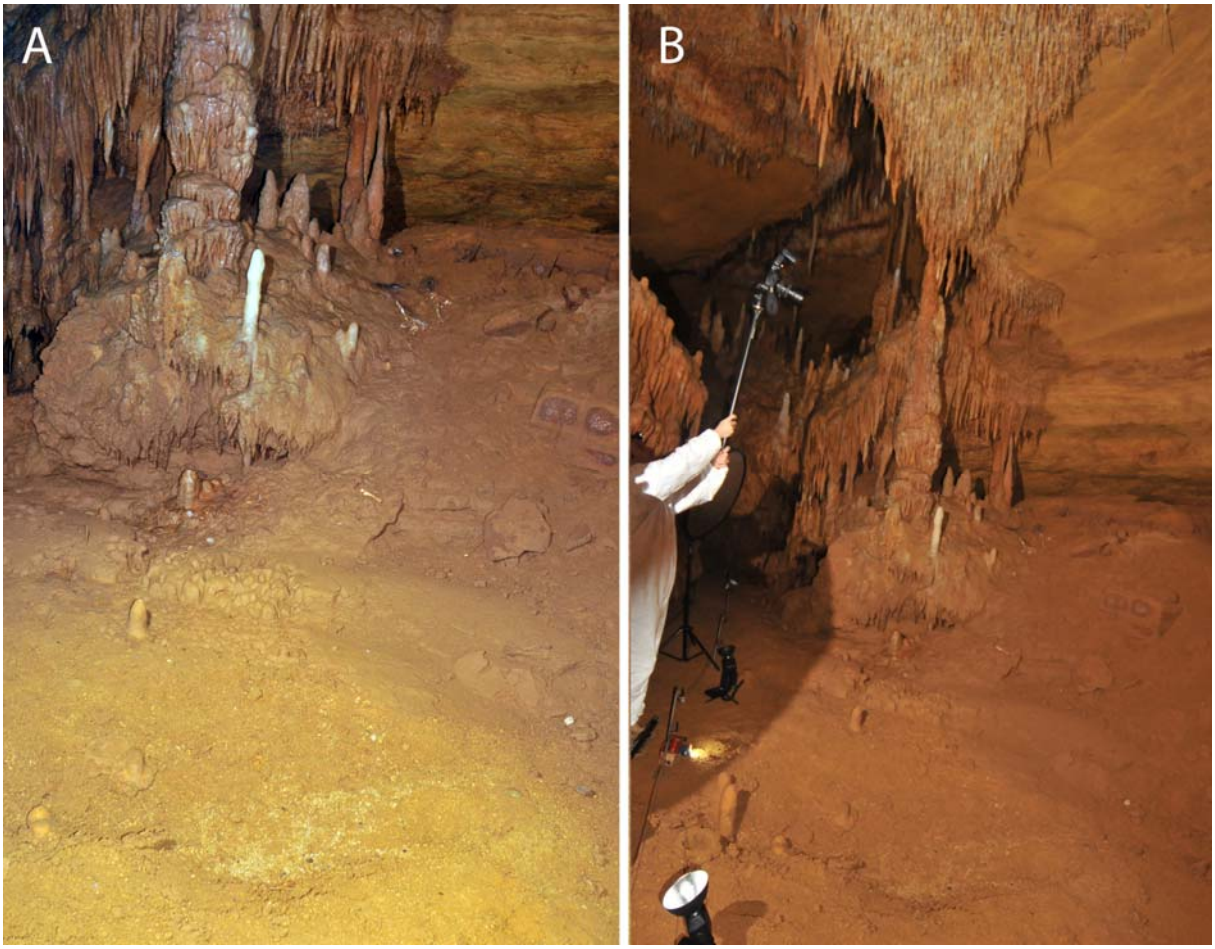

Figure S3. Locus 3. General view from the path (A) and an example of photographic acquisition (B).

In situ analysis

In January 2014, the anthropological team received authorization to remove a portion of the sediment that covered some of the bones of the Locus 2-D1 in order to undertake a study of the skeleton *in situ*: the dental arcades, the spheno-occipital synchondrosis region, the lateral aspect of the right iliac blade and the medial surface of the left coxal bone (including the auricular surface) (Fig. S4). Measurements of the coxal bones and of some long bones were taken using calipers, a cephalometer and a tape measure, without moving the bones and with the aim to leave no marks on them, on their covering, or on the bottom of the nest (3). In January 2016, further observations were made after the removal of sediment of the anterior aspect of a lower lumbar vertebra and the sternal extremity of the right clavicle.

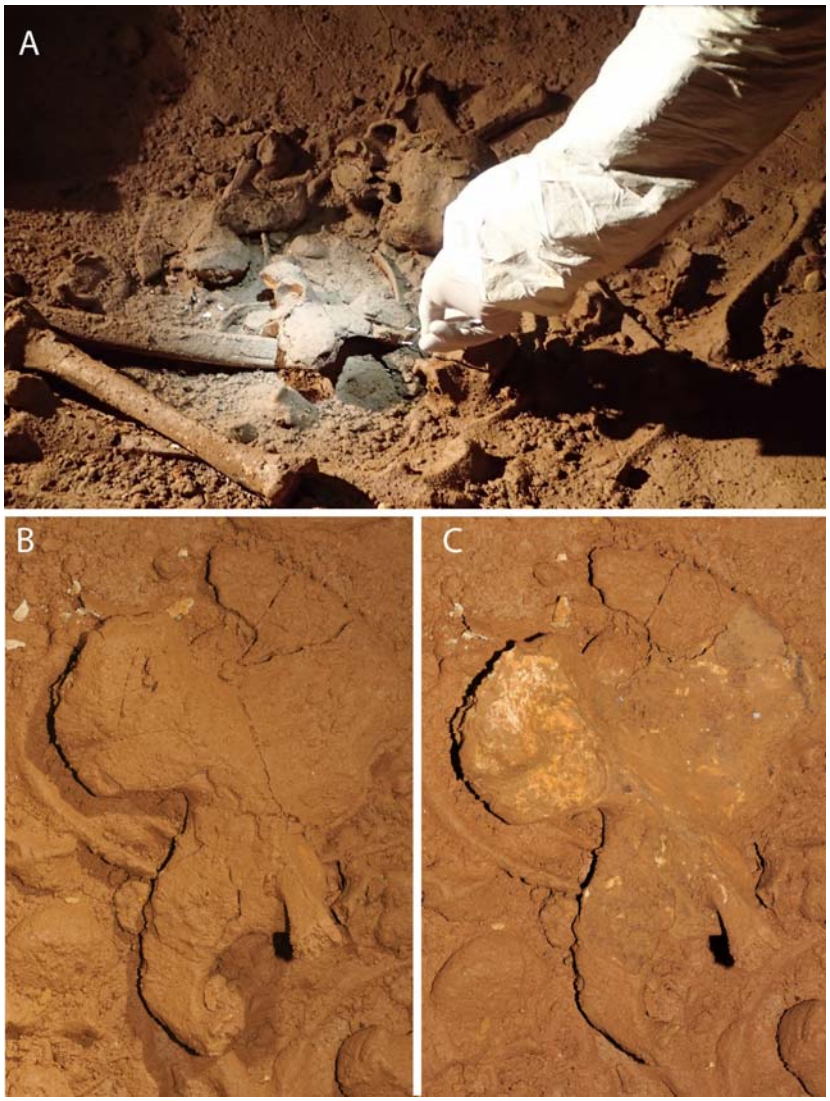

Figure S4. A) Locus 2 *in situ* intervention in 2014. Left coxal bone before (B) and after (C) the partial cleaning.

Virtual analysis

Photographs were processed using our custom photogrammetric solutions based on Bundler and PMVS programs (5,6) and, since 2014, Photoscan (Agisoft©) to compute high definition photogrammetric 3D models. This resulted in several 3D point clouds with a spatial resolutions ranging from 1.0 to 0.5 mm. Points clouds were meshed (using 3Dsystems software) and scaled using local physical scales and topographic points (with x, y, z coordinates, acquired by a Leica© total station). After calibration, the models were exploited in polygon file format (.ply), which allows for the storage of both shape and texture (Fig. S5). The different human bones were virtually extracted from the global models of the loci in order to allow for their detailed study in a virtual environment. The validity of the virtual measurements obtained was tested for the

individual from Locus 2 (2). Comparisons between data obtained *in situ* on the coxal bones of this subject and those obtained from the 3D models indicated a negligible measurement uncertainty: on average 2.4% ± 2.2%; min: 0.01%; max: 7.9% (2).

Figure S5. Illustration of the high definition 3D photogrammetric model of L1-D2.

Sampling

Since the discovery of the Grotte de Cussac, only 10 human bones or fragments of bone have been collected. Six (two from each locus) were collected in 2001 in order to obtain direct ^{14}C dates and to extract ancient DNA from each locus (7). The same year, two bones embedded in the path and located near Locus 1, a very fragmented diaphysis and a complete patella (Fig. S6), were also extracted from the cave. In 2014, a complete left humerus, that rested isolated at the base of the Locus 3 close to the path, was collected (Fig. S6). It was analyzed in the laboratory, scanned via microCT, and reintroduced in the cave in 2017 (8). Finally, in 2019, a fragment of a left mandibular ramus was sampled from Locus 2 in order to attempt a collagen extraction. Unfortunately, the amount of preserved collagen was too low for ^{14}C dating.

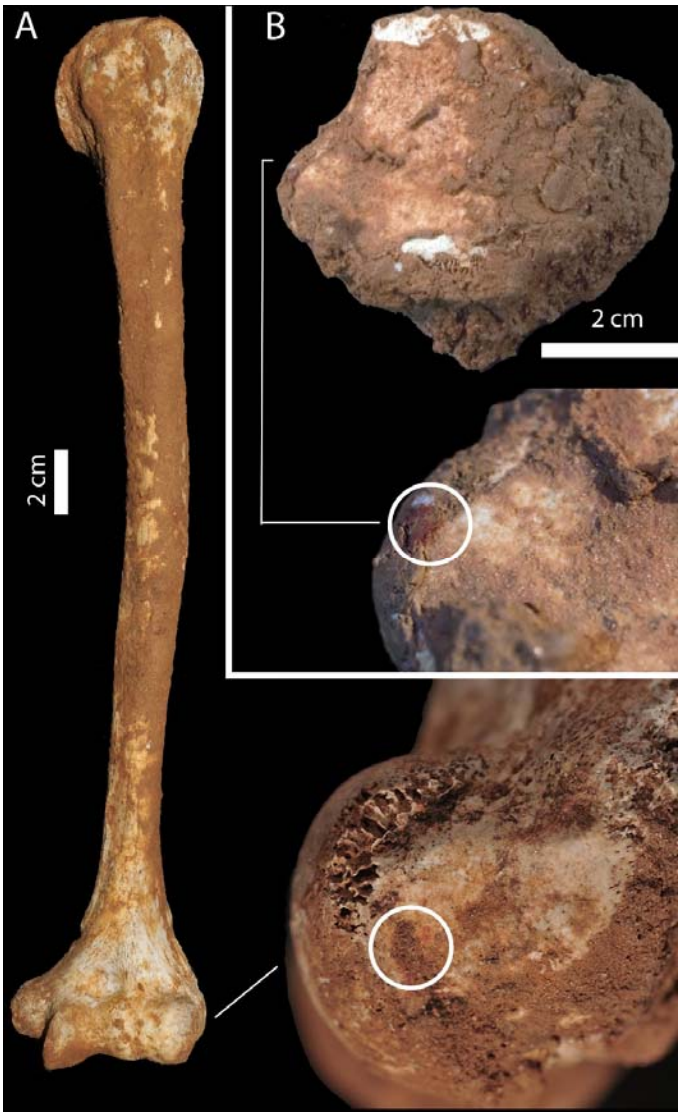

Figure S6. A) Humerus L3-088, collected in 2014. B) Patella L1-090, collected in 2001. Both bones display traces of red pigment.

SI-2: Skeletal inventory of the Loci 1 and 2 area

The skeletal inventories are presented by cluster, following the order that they are found in the text.

Locus 2, Depression 1 (L2-D1)

Forty-seven bones are identified in this area (Table S1). Most of the bones are covered by cave sediment (Fig. S7), making inferences on pigment presence extremely difficult. Moreover, preservation is sometimes difficult to assess due to the fact that some bones are completely embedded.

Table S1. Skeletal inventory for the L2-D1. *: Collected in 2001. Und.: unidentified.

N°	Bone	Side	Preservation
L2-001	Cranium		Complete
L2-002	Mandible		Sub complete
L2-003	Humerus	Right	Complete
L2-004	Humerus	Left	Sub complete or complete
L2-005	Scapula	Left	Sub complete
L2-006	Scapula	Right	Sub complete or complete
L2-007	Rib	Und.	Sub complete or complete
L2-008	Clavicle	Right	Fragmented: medial half
L2-009	Coxal bone	Left	Sub complete
L2-010	Coxal bone	Right	Sub complete
L2-011	Sacrum		Sub complete
L2-012	Rib	Right	?
L2-013	Rib	Und.	?
L2-014	Rib	Left	Sub complete or complete
L2-015	Rib	Right	?
L2-016	Femur	Right	Complete
L2-017	Femur	Left	Complete
L2-018	Tibia	Right	Complete
L2-019	Tibia	Left	Complete
L2-020	Fibula	Und.	Sub complete or complete
L2-021	Fibula	Left	Complete
L2-022	Rib	Left	Shaft fragment
L2-023	Thoracic or lumbar vertebra		Fragmented: body
L2-024	Radius	Right	Complete
L2-025	Rib	Right	Sub complete or complete
L2-026*	Rib	Left	shaft fragment
L2-027*	Metatarsal 2	Left	Complete

L2-028	Radius	Left	Sub complete or complete
L2-029	Rib	Und.	?
L2-030	Thoracic vertebra		Sub complete or complete
L2-031	Ulna	Left	Sub complete or complete
L2-032	Mandible	Left	Left condyle
L2-033	Rib	Und.	Shaft fragment
L2-034	Ulna	Right	Complete
L2-035	Thoracic vertebra		Sub complete or complete
L2-036	Rib	Und.	Shaft fragment
L2-037	Rib	Right	Shaft fragment
L2-041	Flat bone	Und.	?
L2-042	Axis		Complete
L2-043	Rib	Right	?
L2-044	Calcaneus	Right	Complete
L2-045	Rib	Right	Sub complete or complete
L2-046	Thoracic or lumbar vertebra		Sub complete
L2-047	Rib	Und.	?
L2-048	Lumbar vertebra		Complete
L2-049	Thoracic vertebra		Sub complete or complete
L2-050	Flat bone	Und.	?

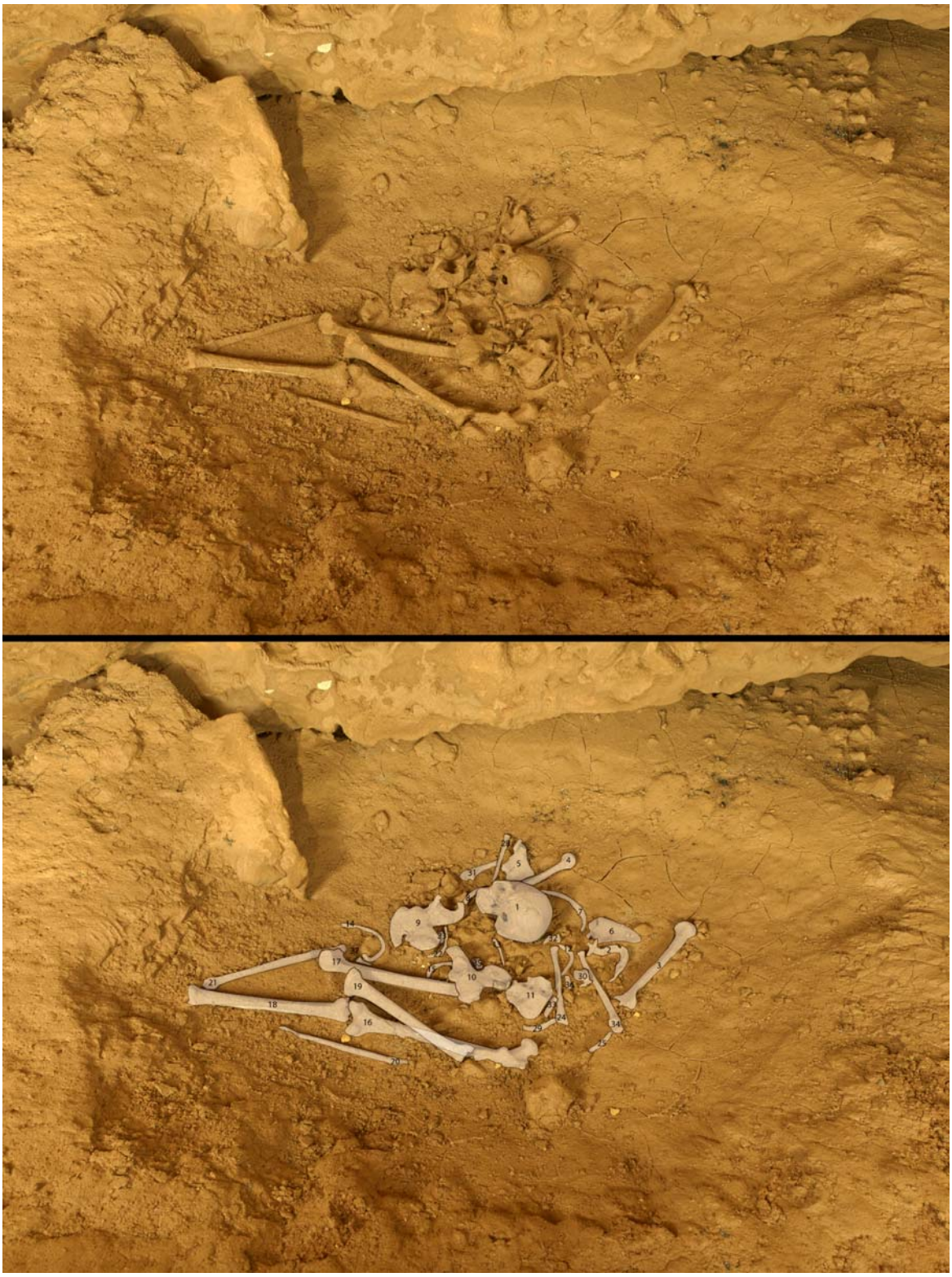

Figure S7. Above: view of L2-D1; below: the same picture with the identified bones grayed out.

Locus 1, Depression 2 (L1-D2)

Contrary to L2-D1, the bones of this cluster are not covered by sediment (Fig. S8). Considering the high degree of fragmentation of the bones in this bear nest, only skeletal elements larger than 5 mm are listed (Table S2); however, a considerable number of smaller bone fragments is visible, forming a bed of fragmentary pieces of bone mixed with sediment (Fig. S8).

Table S2. Skeletal inventory for the L1-D2. *: Elements showing signs of skeletal immaturity. **: Collected in 2001. Und.: unidentified

N°	Bone	Side	Preservation
L1-001*	Femur	Right	Proximal diaphysis and metaphysis
L1-002	Talus	Left	Complete
L1-003	Talus	Right	Complete
L1-004	Talus	Left	Complete
L1-005	Humerus	Und.	Shaft fragment
L1-006	Femur	Und.	Shaft fragment
L1-007	Tibia	Und.	Shaft fragment
L1-008	Pedal Proximal Phalanx	Und.	Complete
L1-009	Thoracic or lumbar vertebra		Body
L1-010*	Metatarsal 3 or 4	Und.	Sub complete
L1-011*	Tibia	Right	Distal epiphysis
L1-012	Humerus	Und.	Shaft fragment
L1-013	Femur	Und.	Shaft fragment
L1-014	Rib	Und.	Shaft fragment
L1-015	Und.	Und.	Fragment
L1-016	Tibia	Und.	Shaft fragment
L1-017	Femur	Und.	Shaft fragment
L1-018	Scapula	Und.	Fragment
L1-019	Sternum		Gladiola
L1-020	Thoracic vertebra		Complete
L1-021*	Femur	Und.	Proximal epiphysis
L1-022	Radius	Right	Proximal third
L1-023	Manual Phalanx	Und.	Sub complete (shaft)
L1-024*	Tibia	Right	Proximal epiphysis
L1-025	Lumbar vertebra		Complete
L1-026	Humerus	Right	Sub complete (head missing)
L1-027	Und.	Und.	Fragment
L1-028	Femur	Und.	Shaft fragment
L1-029	Femur	Und.	Shaft fragment
L1-030	Mandible		Symphysis and left corpus with 7 teeth preserved

L1-031	Patella	Right	Complete
L1-032	Manual Phalanx	Und.	Complete
L1-033	Manual intermediate Phalanx	Und.	Complete
L1-034	Lumbar vertebra		Body
L1-035	Metatarsal 1 or 2	Und.	Distal third
L1-036*	Manual Phalanx	Und.	Complete
L1-037	Flat bone	Und.	Fragment
L1-038	Inferior Premolar	Und.	Complete
L1-039	Flat bone	Und.	Fragment
L1-040	Thoracic vertebra		Body
L1-041	Cervical vertebra		Complete
L1-042	Radius	Und.	Shaft fragment
L1-043	Axis		Sub complete
L1-044	Fibula	Und.	Shaft fragment
L1-045	Fibula	Und.	Shaft fragment
L1-046	Thoracic vertebra		Body
L1-047	Long bone	Und.	Fragment of extremity
L1-048	Thoracic or lumbar vertebra		Complete
L1-049*	Thoracic vertebra		Sub complete
L1-050	Thoracic or lumbar vertebra		Body
L1-051	Long bone	Und.	Fragment of extremity
L1-052	Und.	Und.	Shaft fragment
L1-053	Metacarpal 1?	Und.	Distal half
L1-054	Metatarsal 5?	Und.	Sub complete
L1-055	Femur	Und.	Proximal extremity
L1-056	Femur or Tibia	Und.	Shaft fragment
L1-057	Humerus	Und.	Shaft fragment
L1-058	Femur or Tibia	Und.	Shaft fragment
L1-059	Long bone	Und.	Shaft fragment
L1-060	Long bone	Und.	Shaft fragment
L1-061	Long bone	Und.	Shaft fragment
L1-062	Long bone	Und.	Shaft fragment
L1-063	Long bone	Und.	Shaft fragment
L1-064	Long bone	Und.	Shaft fragment
L1-065	Long bone	Und.	Shaft fragment
L1-066	Metatarsal 4 or 5	Und.	Complete
L1-067	Long bone	Und.	Shaft fragment
L1-093	Lunate	Und.	Complete
L1-094	Radius or Ulna	Und.	Shaft fragment
L1-095	Metacarpal 1	Und.	Sub complete
L1-096	Rib	Und.	Shaft fragment
L1-097	Rib	Und.	Shaft fragment
L1-098	thoracic vertebra		Fragment

L1-099	Inferior canine	Und.	Sub complete
L1-100	Inferior incisor (lateral?)	Right	Complete
L1-102	Inferior canine or Incisor	Und.	Sub complete
L1-103**	Rib	Left	Sub complete
L1-104**	Manual proximal phalanx	Und.	Complete

Figure S8. View of L1-D2, with grayed out bones identified below.

Figure S9. View of L1-D2 at a different angle, with smaller bones grayed out and identified below.

Locus 1, Depression 3 (L1-D3)

Only teeth (no bones) are identifiable in this bear nest (Table S3). However, a dozen of localized spots of white powder, possibly deriving from degraded bone, have been recognized but are not listed here (Fig. S10).

Table S3. Skeletal inventory for the L1-D3. *: Elements showing signs of skeletal immaturity.

N°	Bone	Side	Preservation
L1-068	Upper canine	Und.	Complete
L1-069	Upper premolar 1	Und.	Sub complete
L1-070	Upper incisor	Und.	Sub complete or complete
L1-071*	Upper molar 3	Left	Complete (only crown formed)
L1-072	Upper premolar 2	Und.	Complete?
L1-073*	Upper Molar (2?)	Right?	Complete (root partially formed)
L1-074	Upper Molar (1?)	Right	Complete

Figure S10. Left: view of L1-D3; right: same picture with identified teeth grayed out.

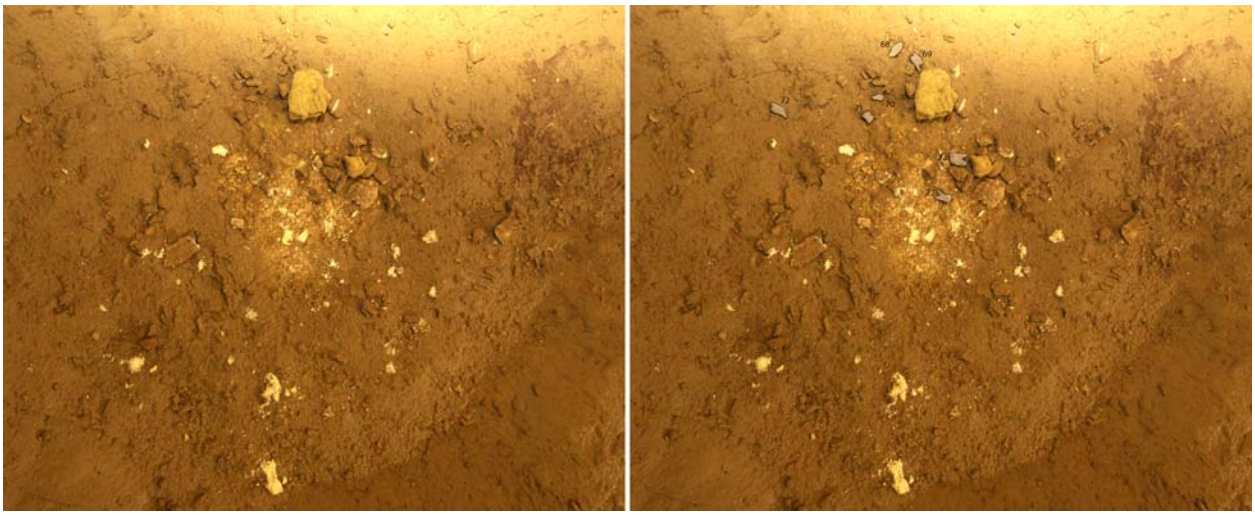

Isolated bones in L1-L2 area

Outside of the bear nests, nine isolated human bones are scattered in the Loci 1-2 area (Table S4).

Table S4. Skeletal inventory of the isolated bones. *: collected in 2001. **: red pigment on the bone.

N°	Bone	Side	Preservation
L1-087	Und.	Und.	Fragmented
L1-088	Thoracic vertebra		Complete
L1-089	Und.	Und.	Fragmented
L1-090	Patella*,**	Left	Complete
L1-091	Thoracic vertebra		Neural arch
L1-092	Rib	Und.	Sub complete or complete
L2-038	Cuboid	Left	Complete
L2-039	Lumbar vertebra		Body
L2-040	Metacarpal 2 or 3	Und.	Complete

SI-3. Skeletal inventory of the Locus 3 area

The skeletal inventories are presented by cluster, following the order they are found in the text.

Locus 3, Depression 1 (L3-D1)

This bear nest contains bone elements that all derive from the lower body (Table S5; Fig. S11). None of them are embedded in sediment. Traces of red pigment are apparent on the bottom and edges of the depression, but not on the bones themselves (Fig. S4).

Table S5. Skeletal inventory for the L3-D1.

N°	**Bone**	**Side**	**Preservation**
L3-001	Und.	Und.	Fragmented
L3-002	Femur	Und.	Proximal extremity
L3-003	Fibula	Right	Complete
L3-004	Lumbar vertebra		Complete
L3-005	Femur	Right	Proximal half of the shaft
L3-006	Coxal bone	Right	Fragment of Ilium
L3-007	Femur	Und.	Shaft fragment
L3-008	Tibia	Und.	Proximal third

L3-009	Und.	Und.	Fragmented
L3-010	Femur	Left	Distal extremity
L3-011	Femur	Und.	Shaft fragment
L3-012	Calcaneus	Right	Complete
L3-013	Talus	Right	Complete
L3-014	Femur	Und.	Proximal extremity
L3-015	Femur	Und.	Distal extremity
L3-016	Und.	Und.	Fragmented
L3-017	Und.	Und.	Fragmented

Figure S11. Top: view of L3-D1; bottom: same picture with identified bones grayed out.

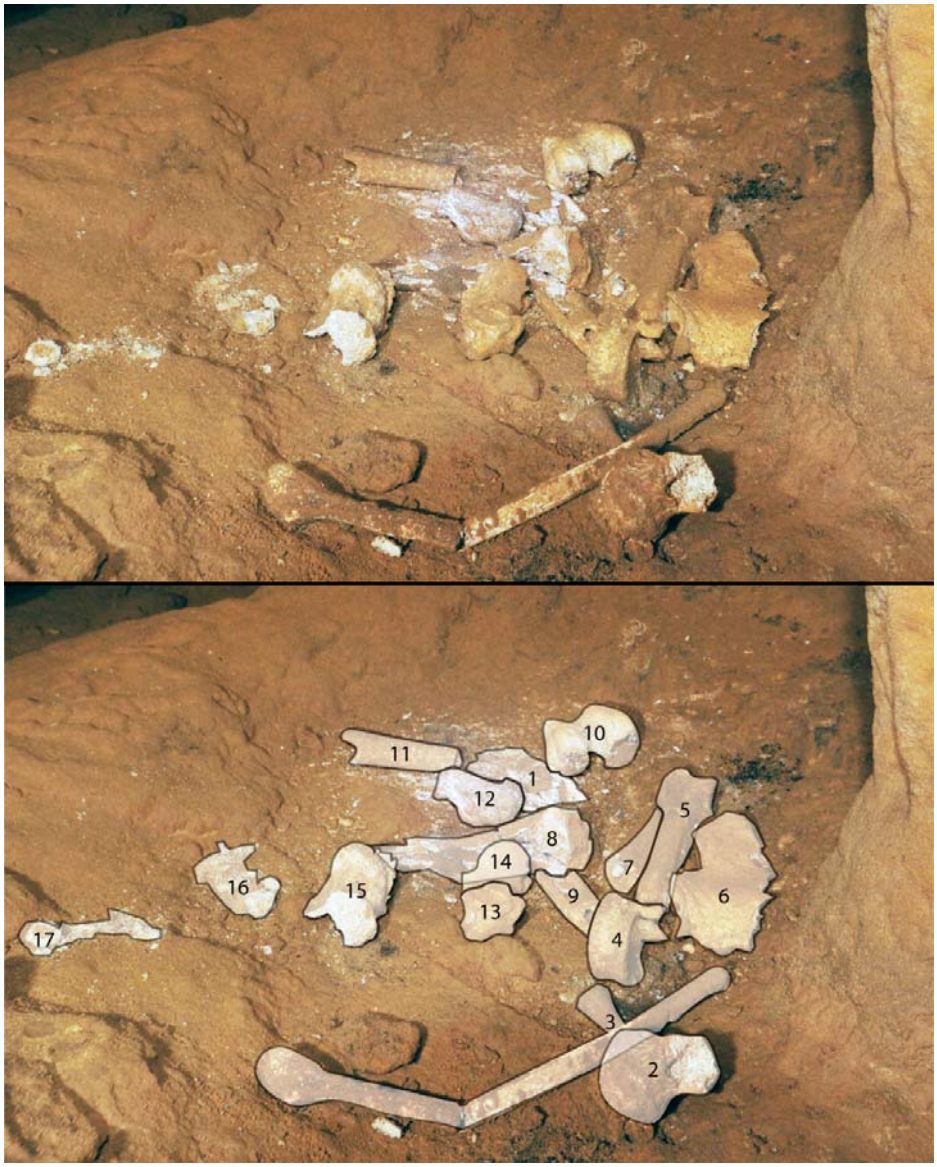

Locus 3, Top Slope (L3-TS)

This cluster contains skeletal elements partially embedded in cave sediment (Fig. S12), some of which show clear signs of skeletal immaturity (Table S6).

Table S6. Skeletal inventory for the L3-TS. *: Element showing signs of skeletal immaturity.

N°	Bone	Side	Preservation
L3-018*	Ulna	Right	Complete
L3-019	Lumbar vertebra		Body
L3-020*	Radius	Right	Complete
L3-021	Lumbar vertebra (5?)		Sub complete or complete
L3-022	Rib	Und.	Fragmented
L3-023	Scapula	Right	?
L3-024*	Humerus	Right	Complete
L3-025	Und.	Und.	Fragmented
L3-090	Pisiform	Right?	Sub complete or complete
L3-091	Triquetrum	Right?	Sub complete or complete
L3-092	Hamate	Right	Sub complete or complete
L3-093	Lunate	Right?	Sub complete or complete
L3-094	Capitate	Right?	Sub complete or complete
L3-095	Scaphoid	Right?	Sub complete or complete
L3-096	Trapezius	Right?	Sub complete or complete
L3-097	Metacarpal 1	Right?	Sub complete or complete
L3-098	Metacarpal	Right?	Sub complete or complete
L3-099	Metacarpal	Right?	Sub complete or complete
L3-100	Metacarpal	Right?	Sub complete or complete
L3-104	Und.	Und.	?

Figure S12. Above: view of L3-TS; below: same picture with identified bones grayed out.

Remote clusters on the upper level of Locus 3

These are several remote clusters with human remains, most of them being extremely fragmented, identified on the upper level of Locus 3 (Table S7). None of the human remains are embedded in cave sediment.

Table S7. Skeletal inventory for remote clusters on the upper level of Locus 3.

N°	Bone	Side	Preservation
L3-064	Und.	Und.	Fragmented
L3-066	Und.	Und.	Fragmented
L3-065	Und.	Und.	Fragmented
L3-058	Femur	Left?	Proximal third of the shaft
L3-057	Humerus	Right	Distal half
L3-061	Und.	Und.	Fragmented
L3-062	Und.	Und.	Fragmented
L3-063	Und.	Und.	Fragmented
L3-106	Und.	Und.	Fragmented
L3-101	Lower molar	Und.	Complete
L3-103	Canine	Und.	Complete

Locus 3, Down Slope (L3-DS)

This grouping is constituted by human remains that are visible at intervals down the L3 slope (Fig. S13). These include upper limb elements, axial skeleton remains, and two pieces of mandible (Table S8).

Table S8. Skeletal inventory for L3-DS. *: red pigment that appear to be in direct contact with the bone.

N°	Bone	Side	Preservation
L3-026	Radius	Left	Complete
L3-027	Clavicle	Left	Sub complete
L3-028	Thoracic or lumbar vertebra		Body
L3-029	Rib	Und.	Fragmented
L3-030	Lumbar vertebra		Sub complete or complete
L3-031	Mandible		Right hemimandible
L3-032	Rib	Und.	Fragmented
L3-033	Rib	Und.	Fragmented
L3-034	Rib	Und.	Sub complete or complete
L3-035	Rib	Und.	Fragmented
L3-036	Rib	Left	Sub complete or complete

L3-037	Und.	Und.	Fragmented
L3-038	Und.	Und.	Fragmented
L3-039	Und.	Und.	Fragmented
L3-040	Und.	Und.	Fragmented
L3-041	Und.	Und.	Fragmented
L3-042	Und.	Und.	Fragmented
L3-043	Thoracic vertebra		Complete
L3-044	Rib	Und.	Fragmented
L3-045	Und.	Und.	Fragmented
L3-046	Humerus	Left	Proximal third
L3-047	Humerus	Right	Complete
L3-048	Metacarpal 3	Left	Complete
L3-049	Ulna	Und.	Shaft fragment
L3-050	Und.	Und.	Fragmented
L3-051	Und.	Und.	Fragmented
L3-052	Und.	Und.	Fragmented
L3-053	Und.	Und.	Fragmented
L3-054	Und.	Und.	Fragmented
L3-055	Rib	Und.	Fragmented
L3-056	Rib 1 or 2	Und.	Complete
L3-059	Metacarpal 3	Und.	Sub complete
L3-060	Und.	Und.	Fragmented
L3-067	Humerus	Left	Distal extremity
L3-068*	Ulna	Right	Proximal third
L3-069	Und.	Und.	Fragmented
L3-070	Clavicle	Left	Sub complete or complete
L3-071	Thoracic vertebra		Complete
L3-072	Mandible		Left hemimandible
L3-073	Manual proximal phalanx	Und.	Complete
L3-074	Rib	Left	?
L3-075	Rib	Und.	Fragmented
L3-076	Rib	Und.	Fragmented
L3-077	Manual Phalanx	Und.	Fragmented
L3-080	Rib	Right	Complete
L3-081	Rib 2 or 3	Right	?
L3-082	Thoracic vertebra		Complete
L3-083	Cervical vertebra		Complete
L3-086	Radius	Right	Complete
L3-087	Lumbar vertebra		Body
L3-105	Manual Phalanx	Und.	Complete

Figure S13. Middle: general view of the L3 slope. Left and right, close up views of bone clusters with identified bones grayed out.

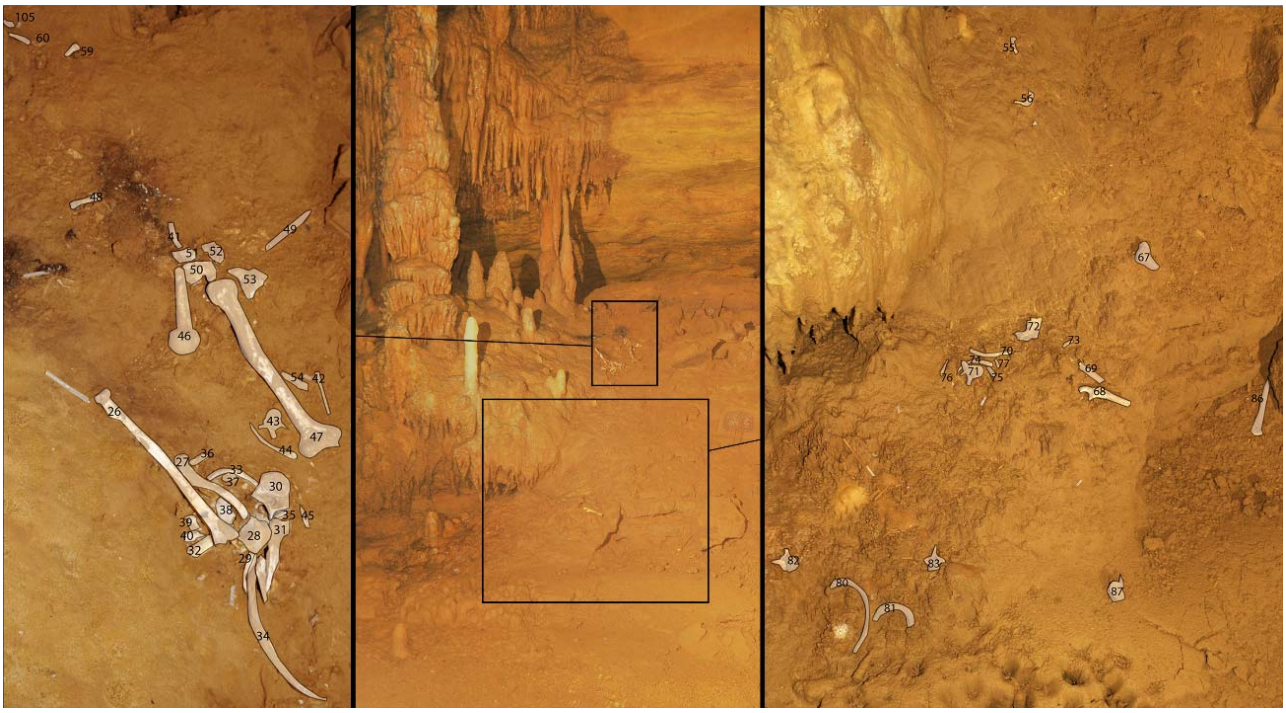

Locus 3: Isolated remains at the bottom of the slope

Isolated remains at the lower level of the slope, in front of the L3, not covered by sediment, and thus likely to have recently fallen from the upper level (Table S9).

Table S9 . *: Collected in 2014 and reintroduced in 2017. **: Traces of red pigment.

N°	Bone	Side	Preservation
L3-084	Und.	Und.	Fragmented
L3-085	Lumbar vertebra		Body
L3-088*, **	Humerus	Left	Complete
L3-089	Manual intermediate phalanx	Und.	Complete

SI-3. Age and Sex Assessments of Identified Individuals

The L1-L2 and L3 areas contain skeletal elements that can be attributed to a minimum of six individuals, including two adolescents (L1A and L3A) and four adults (L1B, L2A, L3B and L3C). This section provides the paleobiological assessment of the ages-at-death, and where applicable sexes, of these individuals.

Individual L1A

Of the various skeletal elements clustered in the L1-D2 depression, some can be confidently attributed to a non-adult individual (Table S10). Based on the dimension of these bones and the nonunion of their epiphyses, they likely all belong to the same younger adolescent, no older than 16 years at the time of death. This is well in accordance with the age estimation based on the maximum width of the tibia proximal epiphysis L1-024 (73.7 mm), i.e. 16.5 ± 4.3 years (9).

Table S10. Inventory of the bones from L1-D2 showing signs of skeletal immaturity, and their estimated age based on epiphyseal union stage (for combined sex).

Label	Bone	Assessed epiphysis	Union stage	Age estimate (years)	Method
L1-001	Femur	Head	Nonunion	≤16	(10)
		Greater trochanter	Nonunion	≤16	(10)
		Lesser trochanter	Nonunion	≤16	(10)
L1-010	Metatarsal	Head	Nonunion	≤16	(11)
L1-011	Tibia	Distal epiphysis	Nonunion	≤18	(10)
L1-021	Femur	Head	Nonunion	≤16	(10)
L1-024	Tibia	Proximal epiphysis	Nonunion	≤18	(10)
L1-036	Manual phalanx	Proximal epiphysis	Nonunion	≤16	(11)
L1-049	Thoracic vertebra	Annular ring	Nonunion	≤20	(11)

The nearby L1-D3 depression contains seven maxillary teeth, including two non-fully mineralized molars (Table S11). Based on their maturation stage (12), these dental elements belong to a non-adult individual, whose age-at-death is between 11 and 14 years. Additionally, four fully mineralized teeth exhibit unworn crowns (upper canine L1-068, upper premolar L1-069, upper incisor L1-070 and first upper molar L1-074), suggesting they may be from the same immature individual. The estimated dental age of this adolescent corresponds well with the degrees of epiphyseal maturation of the bones in L1-D2.

Table S11. Age estimation of the non-fully mineralized teeth from L1-D3. * Estimates according to the *London Atlas of Human Tooth Development and Eruption* (12). Crc: crown completed with defined pulp roof; R3/4: three quarters of the crown length developed.

Label	Tooth	Maturation stage	Age estimate (years)*		
			Min age	Max age	Median
L1-071	Upper molar 3	Crc	11.00	18.99	15.00
L1-073	Upper molar (2?)	R3/4	11.00	14.99	13.00

The most parsimonious hypothesis is to consider the partial bone remains mixed into the bone cluster in L1-D2 and most of the teeth in L1-D3 as derived from the same younger adolescent (L1A), who was 11 to 14 years old at the time of death.

Individual L1B

Apart from the bones of the adolescent L1A, cluster L1-D2 contains various skeletal elements of a second individual (L1B), which differ from the former's by both their size and stage of skeletal maturity. Where preserved, the epiphyses of these bones appear to be fused, in particular the distal epiphysis and medial epicondyle of the humerus L1-026, the femoral head L1-054, and the epiphyses of several metacarpals (L1-053, L1-095), metatarsals (L1-035, L1-054), as well as manual (L1-032, L1-033) and pedal phalanges (L1-008). In addition, numerous vertebral elements have their annular rings fused (L1-020, L1-025, L1-034, L1-040, L1-041, L1-043, L1-046, L1-048). Complete epiphyseal union in these various elements is consistent with their attribution to a single adult (20+ years) individual (11). The partial mandible L1-030, which retains 7 fully erupted permanent teeth (from the right central incisor to the right second molar), is probably from the same individual considering the full mineralization of the roots of the second molar (observable due to taphonomic breakage of the bone) and moderate wear of the tooth crowns. One of the teeth in L1-D3 (the upper premolar L1-072) shows a degree of dental attrition similar to the one observed in these mandibular teeth, in contrast with the other, unworn teeth in that depression. This suggest that this premolar more likely belongs to the adult individual L1B.

Complete fusion of all preserved epiphyses and moderate tooth wear suggest a minimum age in the early 20s for this individual (11). Poor preservation of the remains and the absence of key skeletal regions (such as the auricular surface of the ilium or pubic symphysis) preclude a more accurate estimation of age-at-death. Due to the absence of any sexually-dimorphic skeletal element (coxal bone or cranium), the sex of the individual cannot be assessed.

Individual L2A

The better-preserved remains of individual L2A have been the focus of a detailed paleobiological study, the results of which are presented in detail elsewhere (2,3). The removal of a portion of the sediment in which the bones are imbedded (see SI-1) made it possible to use several indicators to estimate age-at-death, including dental wear, closure of the spheno-occipital synchondrosis (11), fusion of the epiphyses of the long bones and iliac crest (11), and metamorphosis of the auricular surface of the ilium (13). All of the permanent teeth appear to be fully erupted, including the upper and lower third molars. All observable dental crowns are worn, with moderate to large dentine exposure, but without a severe loss of crown height. While some teeth were lost postmortem (mandibular canines, upper central incisors and left upper third molar), there is no evidence of antemortem tooth loss. The spheno-occipital synchondrosis appears to be closed, and the epiphyses of the major long bones are apparently fused. The left iliac crest is fused, without any remnant of the demarcating line between the crest and the iliac blade. All these indicators suggest a minimum age in the late second decade. The examination of the cleaned up auricular surface of the left ilium allows for this estimate to be slightly refined. According to Schmitt's method (13), remodeling stage is indicative of an age-at-death of between 20 and 49 years (with a posterior probability of 98%).

Sex of the individual was assessed based on the morphology (14) and morphometrics (15) of the coxal bones. The first of these approaches did not allow for a secure sex assignment of the individual, as the coxal bones display both male and female features. Measurements taken on the left coxal bones permit to calculate the probability of L2A of being a male or female, by comparing them with those from a worldwide database (15). Result indicates that the individual can confidently be considered as a male (posteriori probability greater than 95%).

Individual L3A

Of the various disconnected skeletal elements present in Locus 3, three bones clustered together on the top of the slope (L3-TS) show clear signs of skeletal immaturity (Table S12). These immature bones share a similar morphology and compatible skeletal maturation stages. In addition, study of the 3D models of these bones indicates that they have compatible maximum dimensions and shows a good articular congruence between the radius and the ulna (4). These three bones therefore likely belong to the same right upper limb of a non-adult individual in its second decade of life. Considered together, the stages of epiphyseal fusion of these three long bones indicate an age-at-death of between 16 and 21 years, with a 97% posterior probability (16) (Fig. S14).

Table S12. Inventory of the bones from Locus 3 showing signs of skeletal immaturity, and their estimated age based on epiphyseal union stage (according to (16), for combined sex).

Label	Bone	Assessed epiphysis	Union stage	Age estimate (years)
L3-018	Ulna	Proximal epiphysis	Complet union	≥13
		Distal epiphysis	Nonunion	≤18
L3-020	Radius	Proximal epiphysis	Complete union	≥11
		Distal epiphysis	Nonunion	≤18
L3-024	Humerus	Head	Partial union	14-21
		Medial epicondyle	Complete union	≥11
		Distal epiphysis	Complete union	≥11

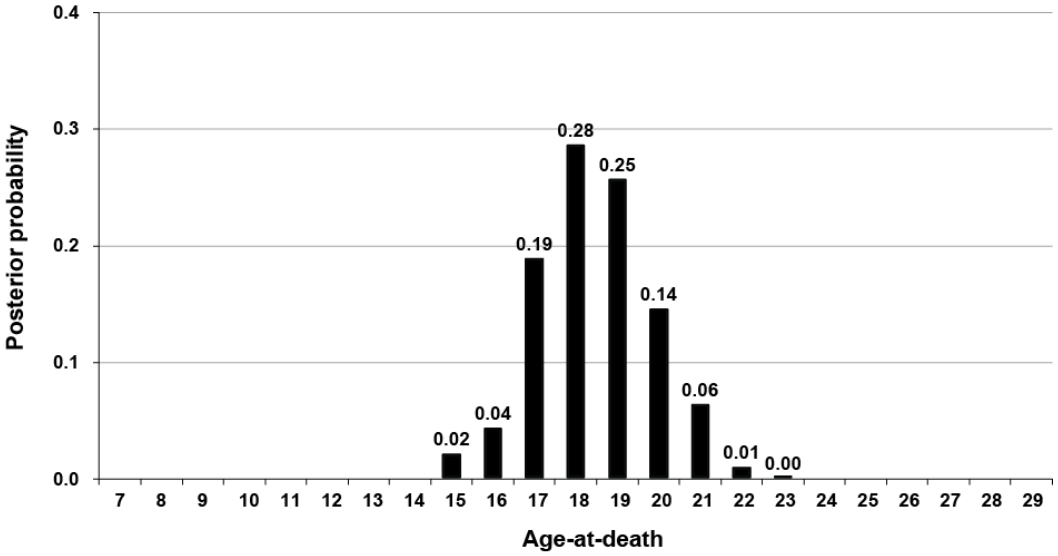

Figure S14. Distribution of the posterior probabilities of age-at-death of individual L3A, based on the stage of epiphyseal union of the right humerus, radius and ulna (4).

Apart from these three bones, other skeletal elements can be attributed to individual L3A. The right scapula L3-023 and the 11 right hand bones located in the cluster L3-TS possibly are from the same upper limb. The 3D model of left humerus L3-067, represented by its distal end, articulates relatively well with the mirrored 3D models of the right radius L3-020 and right ulna L3-018, making it probable that this bone belongs to individual L3A (4). It is possible that the right coxal bone L3-006 also belongs to this individual, given its small size when compared to those of known Gravettian adults (4), which suggest that this bone had possibly not fully completed its growth.

Individual L3B

In addition to individual L3A, two other subjects are identified in the Locus 3 area. The first one (L3B) is represented by the complete left humerus L3-088, as well as few other bones that can be associated with it based on the study of their 3D models (4). The pair of radii L3-026 and L3-86 probably belongs to this individual, considering that the maximum length of left radius L3-026 fits with the maximum length of humerus L3-088, while is incompatible with the ones of the other humeri in Locus 3. An attribution to this individual is also probable for the ulna L3-086, of which the mirrored 3D model shows a very good articular congruence with humerus L3-088. The allocation of two more bones to this individual (right fibula L3-003 based on its maximum length and right humerus L3-057 by exclusion) is also possible but cannot be ascertained.

All of these bones show complete union of their epiphyses. Individual L3B is therefore most likely an adult, whose sex cannot be assessed due to the absence of any sexually-dimorphic skeletal element (coxal bone or skull).

Individual L3C

Individual L3C is represented by a single bone, the right humerus L3-047. This bone seems very robust, with a short maximum length. The association of this bone with left humerus L3-088 (L3B) is unlikely, given their major difference in shape and significant difference in size (4). Humerus L3-047 show complete union of all epiphyses (head, distal epiphysis and medial epicondyle). Individual L3C is therefore likely an adult (17), whose sex cannot be assessed.

Age and Sex Summary

The estimated ages-at-death and sex attributions for the six individuals from the Grotte de Cussac are summarize in Table S13.

Table S13. Summary of paleobiological information on the individuals of the Grotte de Cussac.

Individual	Age category	Estimated age	Sex	Reference
L1A	Adolescent	11-14	Not determined	Unpublished
L1B	Adult	20+	Not determined	Unpublished
L2A	Adult	20-49	Male	(2,3)
L3A	Adolescent	16-21	Not determined	(4)
L3B	Adult	20+	Not determined	(4)
L3C	Adult	20+	Not determined	(4)

SI-4. Hypothetic Chains of Events

Schematic representation of the hypothetic chains of events that led to the formation of the main clusters of human remain in the Grotte de Cussac. With the exception of individual L2A, who decomposed in the L2-D1 depression without subsequent anthropic intervention, all of the individuals were subjected to post-mortem manipulations, including bone transfer from the initial place of deposition of the body, the removal of skeletal elements (crania and possibly other bones), and the deliberate commingling of the remains of several individuals together.

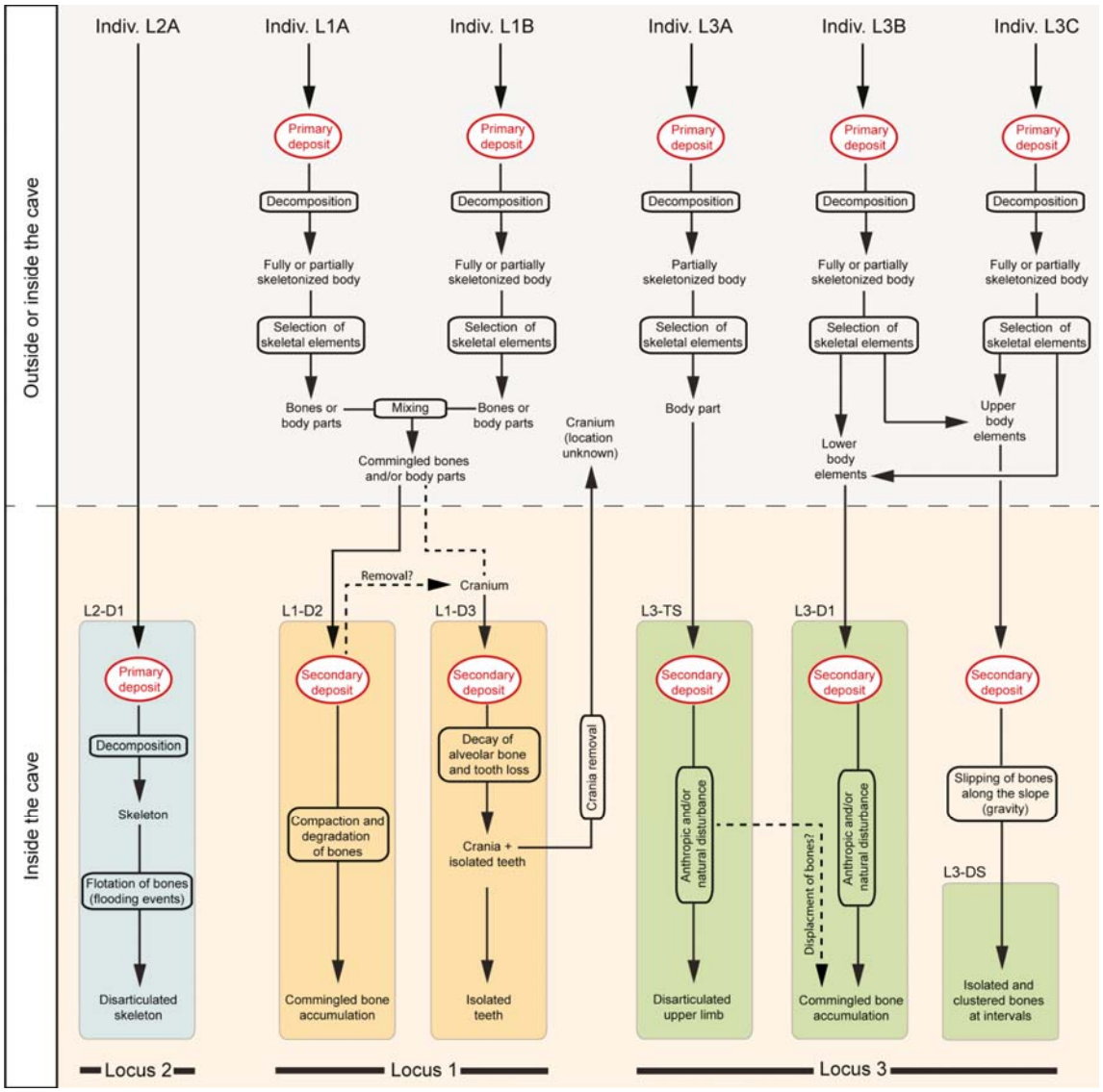

Figure S15. Hypothetic sequences of events regarding the postmortem processes affecting the remains of the identified individuals in the Grotte de Cussac.

SI-5. Abnormalities of Cussac L2A

The exposed remains of the Cussac L2A individual do not reveal any apparent abnormalities, but the individual is nonetheless unusually small for a Eurasian Mid Upper Paleolithic (MUP) young adult male (2,3) (see age and sex assessment above). The estimated bicondylar femoral length of ≈447 mm is only 1.41 standard deviations below a male MUP mean, but the humeral maximum length of ≈300 mm is 2.23 standard deviations below a respective mean (Fig. S16). The femoral head diameter (≈41.3 mm), predicted from its acetabular height of 50.1 mm, falls below the smallest Gravettian male (Předmostí 9: 42.0 mm) and is 2.29 standard deviations from the male mean.

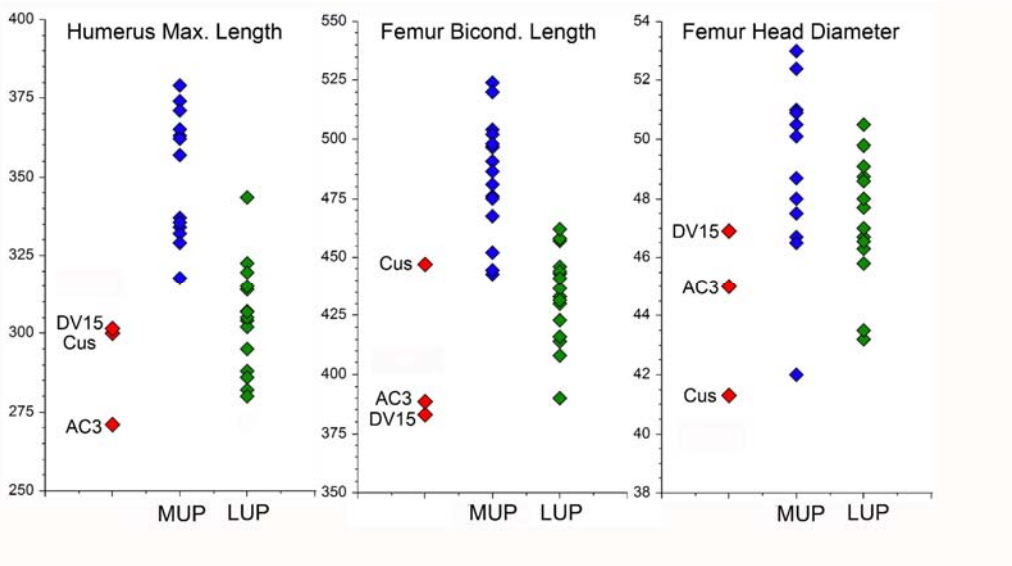

Figure S16. Limb length (humerus and femur lengths) and body mass (femoral head diameter) indications for Cussac L2A (Cus) and other European Upper Paleolithic individuals. MUP: Mid Upper Paleolithic; LUP: Late Upper Paleolithic; AC3: LUP Arene Candide 3; DV15: MUP Dolni Věstonice 15. Arene Candide 3 and Dolni Věstonice 15 exhibit developmental dysplasias (18,19).

The body proportions of Cussac L2A are also at the limits of the known MUP variation (Fig. S17). His crural (tibio-femoral) and humero-femoral indices (81.7 and 67.1 respectively; both using femoral bicondylar length), are among the lowest Gravettian values (81.1 for Veneri 2, and 67.4 for Grotte-des-Enfants 5 respectively, both females). His femoral head to length index of ≈9.24 is similarly at the low end of the earlier Upper Paleolithic values, exceeding only that of the female Grotte-des-Enfants 5 (9.14).

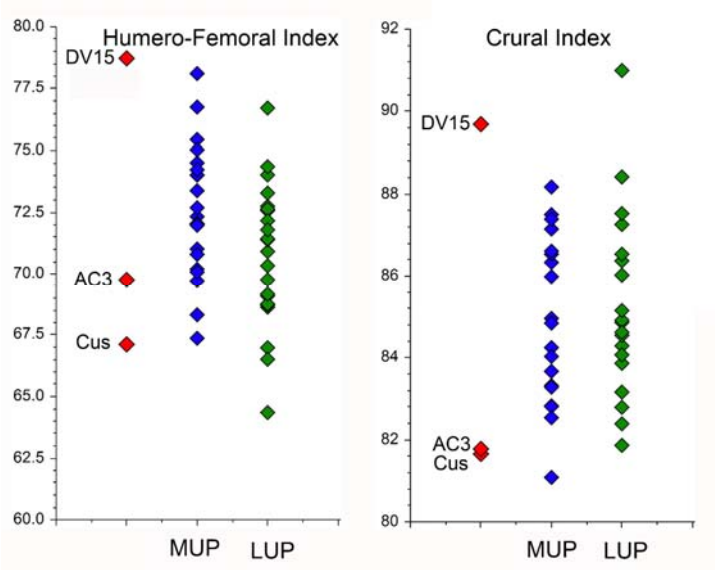

Figure S17. Upper versus lower limb (humero-femoral) and lower limb segment (crural; tibio-femoral) proportions for Cussac L2A (Cus) and other European Upper Paleolithic individuals. Abbreviations as in Fig. S16.

As previously documented (2,3), and evident here, the Cussac L2A individual is at or slightly beyond the known limits of Gravettian males in terms of body size and Gravettian males and females in body proportions. It remains uncertain whether this individual was merely a short Gravettian male or his size and proportions reflect developmental abnormalities; in either case Cussac L2A is unusual for his context.

SI-6. Supporting Information References

1. N. Fourment, D. Barraud, M. Kazmierczak, A. Rieu, “La grotte de Cussac (Le Buisson-de-Cadouin, Dordogne, France) : applications des principes de conservation préventive au cas d’une découverte récente” in *L’art Pléistocène Dans Le Monde/Pleistocene Art of the World/Arte Pleistoceno En El Mundo. Actes Du Congrès IFRAO (Tarascon-Sur-Ariège, septembre 2010)*, J. Clottes, Ed. (2012), pp. 64–65 (CD-Rom, 343–354).
2. P. Guyomarc’h, *et al.*, New data on the paleobiology of the Gravettian individual L2A from Cussac cave (Dordogne, France) through a virtual approach. *J. Archaeol. Sci. Rep.* **14**, 365–373 (2017).
3. S. Villotte, F. Santos, P. Courtaud, In situ study of the Gravettian individual from Cussac cave, locus 2 (Dordogne, France). *Am. J. Phys. Anthropol.* **158**, 759–768 (2015).

4. C. Peignaux, S. Kacki, P. Guyomarc'h, E. M. J. Schotsmans, S. Villotte, New anthropological data from Cussac Cave (Gravettian, Dordogne, France): In situ and virtual analyses of Locus 3. *C. R. Palevol* **18**, 455–464 (2019).
5. Y. Furukawa, J. Ponce, Accurate, dense, and robust multi-view stereopsis. *IEEE Trans. Pattern Anal. Mach. Intell.* **32**, 1362–1376 (2010).
6. N. Snavely, S. M. Seitz, R. Szeliski, Modeling the World from Internet Photo Collections. *Int J. Comput. Vision* **80**, 180-210 (2008).
7. N. Aujoulat, *et al.*, La grotte ornée de Cussac - Le Buisson-de-Cadouin (Dordogne) : premières observations. *Bull. Soc. Préhist. Fr.* **99**, 129–137 (2002).
8. P. Guyomarc'h, V. Sparacello, M. Samsel, P. Courtaud, S. Villotte, New Biological Data on a Gravettian Humerus from the Cussac Cave (Dordogne, France). *Bull. Mém. Soc. Anthropol. Paris* (2019) https:/doi.org/10.3166/bmsap-2019-0063 (January 9, 2020).
9. E. N. Conceição, H. F. V. Cardoso, "Estimating age at death from the size of the growing epiphyses and metaphyses of the femur and tibia at the knee" in *Acta medicinae legalis et socialis,* D. N. Vieira, A. Busuttil, D. Cusack, P. Beth, Eds. (International Academy of Legal Medicine, 2010), pp. 29-34.
10. H. F. Cardoso, Epiphyseal union at the innominate and lower limb in a modern Portuguese skeletal sample, and age estimation in adolescent and young adult male and female skeletons. *Am. J. Phys. Anthropol.* **135**, 161-170 (2008).
11. L. Scheuer, S. Black, *Developmental Juvenile Osteology* (Elsevier Academic Press, 2000), pp. 592.
12. S. J. AlQahtani, M. P. Hector, H. M. Liversidge, Brief communication: the London atlas of human tooth development and eruption. *Am. J. Phys. Anthropol.* **142**, 481-490 (2010).
13. A. Schmitt, Une nouvelle méthode pour estimer l'âge au décès des adultes à partir de la surface sacro-pelvienne iliaque. *Bull. Mém. Soc. Anthropol. Paris* **17**, 89-101 (2005).
14. J. Brůžek, A method for visual determination of sex, using the human hip bone. *Am. J. Phys. Anthropol.* **117**, 157-168 (2002).
15. P. Murail, J. Brůžek, F. Houët, E. Cunha, DSP: a tool for probabilistic sex diagnosis using worldwide variability in hip-bone measurements. *Bull. Mém. Soc. Anthropol. Paris* **17**, 167-176 (2005).
16. H. Coqueugniot, T. D. Weaver, F. Houët, Brief communication: a probabilistic approach to age estimation from infracranial sequences of maturation. *Am. J. Phys. Anthropol.* **142**, 655-664 (2010).
17. H. F. Cardoso, Age estimation of adolescent and young adult male and female skeletons II, epiphyseal union at the upper limb and scapular girdle in a modern Portuguese skeletal sample. *Am. J. Phys. Anthropol.* **137**, 97-105 (2008).
18. V. Formicola, X-linked hypophosphatemic rickets: a probable Upper Paleolithic case. *Am. J. Phys. Anthropol.* **98**, 403-409 (1995).
19. E. Trinkaus, S.W. Hillson, R.G. Franciscus, T.W. Holliday. 2006. "Skeletal and dental paleopathology" in *Early Modern Human Evolution in Central Europe: The People of Dolní*

Věstonice and Pavlov, E. Trinkaus, J.A. Svoboda, eds (Oxford University Press, 2006), pp. 419-458.